ASSOCIAZIONE NAZIONALE ITALIANA DI INGEGNERIA SISMICA ANIDIS
Italian National Association of Earthquake Engineering

XVIII CONVEGNO ANIDIS
L'ingegneria sismica in Italia
ASCOLI PICENO 2019
15-19 Settembre

Experimental detection of the residual prestressing level in pre-tensioned and post-tensioned reinforced concrete beams by means of non-destructive tests

Michele Frizzarin[a,b], Flora Faleschini[a], Mariano Angelo Zanini[a], Paolo Franchetti[b], Carlo Pellegrino[a]
[a] *Dipartimento di Ingegneria Civile, Edile e Ambientale, Università degli Studi di Padova, Via Marzolo, 35131 Padova, Italy*
[b] *Studio Franchetti srl, P.le della Vittoria 7, 36071 Arzignano, Italy*

Keywords: Prestressed concrete; non-destrucrive tests; dynamic identification; ultrasonic tests

ABSTRACT
Object of the paper is the execution of an experimental campaign conducted on six prestressed concrete beams (PC) and different levels of prestressing. In the first phase, three beams with straight adherent cables were casted, with the same eccentricity and three different levels of prestressing. For each beam, static tests were carried out until failure, and for each load step several non-destructive tests were carried out, namely dynamic free vibration tests and ultrasonic tests. The beams were instrumented with strain gauges and LVDTs to measure deformation and displacements during load cycles. The same tests were then repeated on three further beams with straight post-tensioned cables, with the possibility of controlling the level of prestressing force. In this case, each of the three beams had a different eccentricity. The variation of non-destructive parameters (such as dynamic characteristics and properties of ultrasonic waves) as a function of the degree of prestressing is evaluated, as well as the increase in the structural damage of the element. In particular, dynamic response data were analyzed in both frequency domain and time domain. Ultrasonic response data were also analyzed, not only in terms of velocity but also through attenuation of the ultrasonic signal. The aim of the study is to improve the techniques currently used for the detection of damage of PC elements with non-destructive tests, by defining a new protocol for the evaluation of residual prestressing force through the use of non-destructive tests. This will allow a more detailed assessment of the condition of the structure with a limited amount of data.

1 INTRODUCTION

In the field of civil infrastructures, the conservation of the enormous stock of existing bridges and other civil structures world-wide is an extremely complex issue that involves technical, social, economic and political considerations.

However, while this issue is gaining social attention with time, there is still the need for more research on the topic, in order to improve and/or establish reliable intervention procedures and techniques to carefully assess the actual health condition of structures. As a consequence, there is a lack of an appropriate framework of well-established theoretical schemes and technical tools for the diagnosis and design of such interventions, which would take into account the functional and economic value of any asset, and in general its overall context.

This paper aims at investigating one of the main topics of the structural damage identification, which importance is increasing every year, also driven by recent tragic events: the measure of residual prestressing force in existing prestressed concrete bridges. This is of course one of the fundamental keys for understanding the real health condition of the whole structure. In fact, a substantial difference between the design and the actual prestress force might lead to serviceability and safety impairments (Saiidi et al., 1994). Despite this, unless the bridge is instrumented at the time of construction, the existing prestress force cannot be directly estimated. This is due to the impossibility of directly accessing the prestressing cables, except for the case of external ones.

The problem of prestress force estimation is being tackled since at least 30 years (Tse et al., 1978). The first approach to the problem is related to the well-known method of the measure of the variation in the fundamental frequency of vibration (Cawley and Adams, 1979). The classical formulation for the evaluation of the fundamental frequencies in a prestressed beam-type element, with a centred prestressing load, is

$$\omega_n^2 = -\left(\frac{n\pi}{L}\right)^2 \frac{N}{m} + \left(\frac{n\pi}{L}\right)^4 \frac{EI}{m} \qquad (1)$$

where ω_n is the n-th circular frequency, N is the axial force applied to the beam, m is the mass per unit length in (kg/m), L is the length of the beam and EI is the flexural stiffness. In the case of the first fundamental frequency, Eq.1 becomes:

$$f = \frac{\pi}{2L^2}\sqrt{\frac{EI}{m}\left(1-\frac{N}{N_{cr}}\right)} \qquad (2)$$

where N_{cr} is the Eulerian load.

As it can be seen from Eq.2, the variation in the fundamental frequency of the element depends on the square root of the ratio between the applied prestressing force and the Eulerian load, thus it is expected that the variation on this parameter will be perceptible only for considerable variation of the prestressing force (Dall'Asta and Dezi, 1996). Hence, further parameters should be monitored in order to capture prestress force losses, even with low magnitude of values; such parameters must show high sensitivity to prestress force variation. In the last two decades, several experimental campaigns were carried out aimed to solve this problem, however showing controversial results. Unger et al. (2006) concentrated the study on modal identification without taking into account the variation of prestressing force. Wang et al. (2013), in opposition with previous experimental results, stated that the variation of flexural stiffness of prestressed beams with parabolic tendons decreases with increasing the prestressing force value, while the flexural stiffness of prestressed beams with straight tendons is not being affected by variations of the prestressing force. These considerations were again denied by Toyota et al. (2016), who performed a comprehensive study aimed at taking into account the effects of temperature also.

Other studies used time domain techniques to identify the prestressing force, without considering frequency-based models (Lu and Law, 2005). Lastly, few papers adopted also damping measures (Toyota et al., 2016), showing a general decrement of damping with prestressing force. However, doubts arise about the effective applicability of this method, being in some cases prestress loss effects on damping properties not enough strong to be perceived over the temperature and humidity effects.

2 EXPERIMENTAL CAMPAIGN

The experimental campaign described in the present paper took place at the Laboratory for Construction Materials Tests of the University of Padova. The experimental work relates to six beams, subdivided in two groups. Beam 1, 2 and 3 are characterized by adherent cable prestressed concrete, having different prestress force level. Beam 4, 5 and 6 are characterized by post-tensioned concrete, with cables inserted in plastic ducts, and different eccentricity.

The level of prestressing force (F_p) in the cable is listed in Table 1, together with the gross concrete section area (A_c), the prestressing steel area (A_p), the prestress on the concrete (σ_c) and the cable eccentricity (e_s). For the beams realized with adherent straight cables (1, 2 and 3), F_p was applied before beams casting; for the beams with sliding cables (4, 5 and 6), F_p was regulated through a hydraulic jack during the tests.

Table 1. Main features of the tested beams.

ID	A_c (mm^2)	A_p (mm^2)	F_p (kN)	σ_c (MPa)	e_c (mm)
Beam 1	60000	139	70	1.13	80
Beam 2	60000	139	140	2.27	80
Beam 3	60000	139	190	3.07	80
Beam 4	60000	139	0-160	0-2.67	0
Beam 5	60000	139	0-160	0-2.67	40
Beam 6	60000	139	0-160	0-2.67	80

2.1 *Beams geometry and materials*

All the beams tested here are characterized by the same common features:

- Cross-section: rectangular, with 200 mm (base) x 300 mm (height);
- Element length: 6000 mm;
- Longitudinal steel reinforcement: 4 longitudinal bars, diameter 8 mm, at the 4 corners of the section (concrete cover 25 mm);
- Transverse steel reinforcement: rectangular stirrups, diameter 8 mm, spacing of 100 mm along all the length of the beam; at the support, the spacing is increased at 50 mm in order to avoid shear failure during the static tests;
- Prestressing steel reinforcement: 7 wires single strand, equivalent diameter 6/10", straight disposition. Eccentricity of the strand from 0 mm to 80 mm from the barycentre of the section (150 mm to 70 mm from the bottom of the beam).

Figure 1 shows the geometry of the beams tested here, with steel reinforcement details.

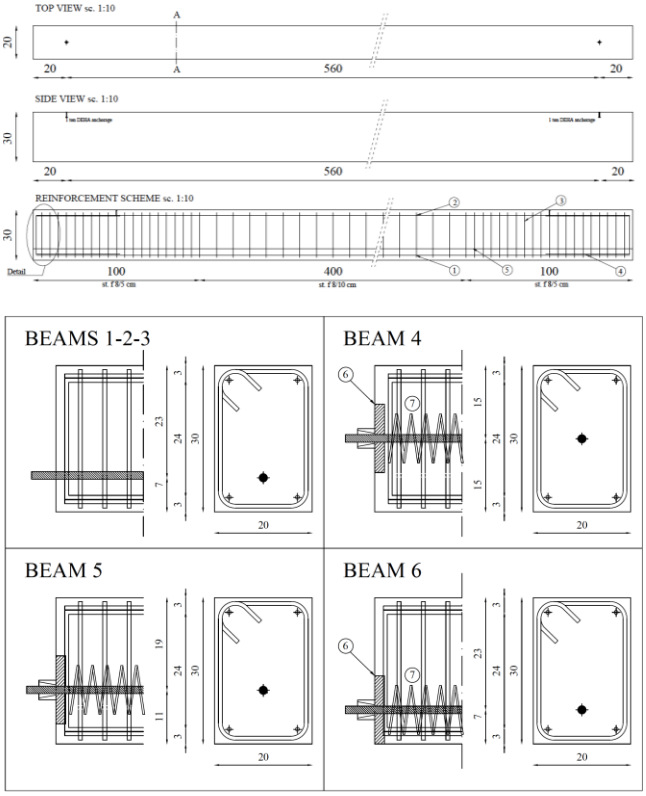

POS.	SHAPING	N°	Ø	cm	Kg
1		2	8	604	4.8
2		2	8	604	4.8
3		156	8	104	64.1

POS.	SHAPING	N°	Ø	cm	Kg
4		4	8	123	1.94
5	HARMONIC STEEL	1	15.2	700	7.63

Figure 1. Beams geometry and reinforcement arrangement.

The beams were cast at the Castelvetro prefabrication plant of RDB Italprefabbricati. Concerning material properties, concrete compressive strength was evaluated on a sufficient number of cube specimens per each beam at the time of testing (about 55 ± 5 days after concreting). Average cube compressive strength values were: 69MPa, 66 MPa and 65.3MPa respectively for Beam 1, 2 and 3; 62.5, 64.5 and 67 respectively for Beam 4, 5 and 6. For the reinforcement, ordinary B450C steel was used, with a nominal yield strength of 450 MPa and a failure strength of 540 MPa. Tensile tests performed on three samples of steel taken from the same production lot provided an average yield strength of 512 MPa, failure strength of 612 MPa and average elongation about 10‰. Lastly, for the prestressing cable, prestressing steel was used with a nominal strength at 1% of total elongation $f_{p(1)k}$ of 1670 MPa and an ultimate strength of 1860 MPa. Tensile tests were then performed on three samples to evaluate experimentally the above properties, on specimens taken from the same production lot. Experimental average results are: $f_{p(1)k}$ of 1703 MPa, f_{pt} of 1925 MPa, ad average elongation of 6.4%.

2.2 *Test setup*

Beams 1, 2 and 3 were subject to four point bending test (4PBD), while Beams 4, 5 and 6 were subjected to three points bending test (3PBD) with a test program that includes a series of load cycles (load-unload) up to the failure. The following static parameters were monitored continuously: vertical displacement along the length of the element, concrete strains at relevant locations, and the vertical force applied. For Beams 4, 5 and 6 also the applied prestressing force was measured. Concerning beam displacement, 5 LVDTs (Linear Variable Differential Transformer) were used, having a precision of ±0.01mm. Concrete strains were monitored by eight sensors positioned along the beam in 4 couples, one at the upper side and one at the lower side of the element, at 25 mm from the upper and lower surface respectively, with the purpose to measure the bending deformation at the beam at significant points. In the case of Beam 1, 2 and 3 the deformations were measured by eight SGs (Strain Gauges), while in the case of Beam 4, 5 and 6 the deformations were measured by eight DD1s (Distortion Detectors). Vertical load was monitored by a load cell with 100kN capacity, and sensitivity of 2mV/V ± 0.1%. In the case of post-tensioned beams, cable load was monitored by two load cells (one at each side of the cable, in order to measure the friction losses) with 600kN capacity, and sensitivity of 2mV/V ± 0.1%. Between one cycle and another, non-destructive tests (NDTs) were carried out. Figure 2 shows the loading setup adopted for Beams 1, 2 and 3 (Figure 2.a) and for Beams 4, 5 and 6 (Figure 2.b). Similarly, Figure 3 shows the disposition of the instrumentation for the two groups of beams.

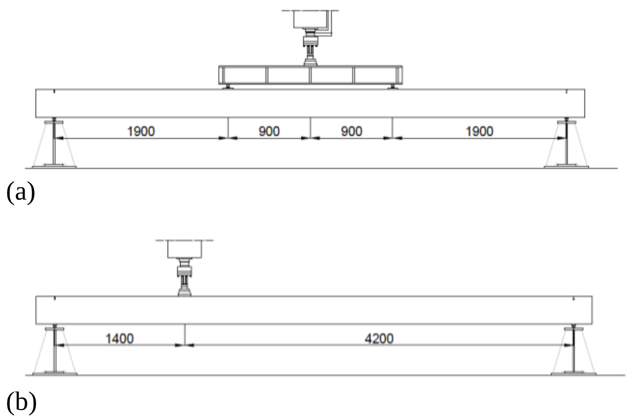

Figure 2. (a) Bending test for Beams 1, 2 and 3: geometry (b) Bending test for Beams 4, 5 and 6: geometry (side-view).

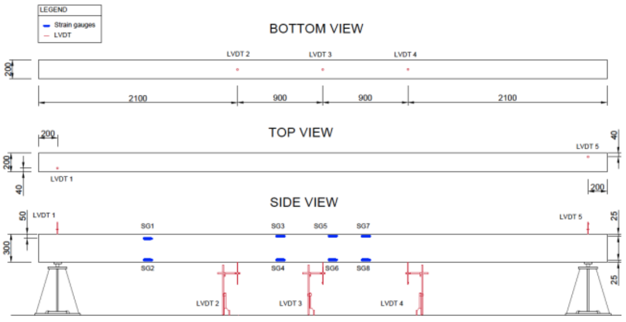

(a)

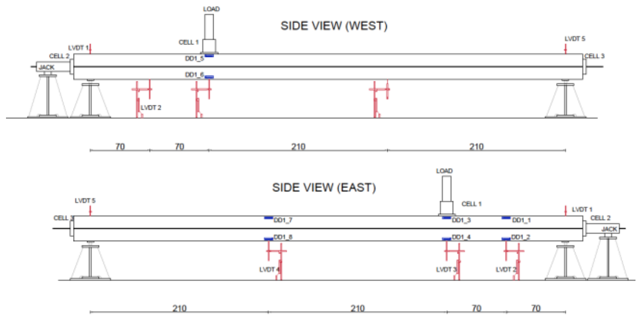

(b)

Figure 3. Location of the instrumentation for beam displacement and concrete strains monitoring (respectively, in red – LVDTs and in blue – SG/DD1). (a) Beams 1, 2 and 3 (b) Beams 4, 5 and 6.

Concerning the applied load cycles, they were as it follows: an incremental load phase, a stationary stage, and then the unloading. During the stationary stage, crack pattern was detected. All the cycles were load controlled. Table 2 shows the load cycles for Beams 1, 2 and 3. In the case of Beams 4, 5 and 6 the load was changed together with precompression level, as shown in Table 3.

Concerning NDTs, they were carried out after each load cycle, in unloaded beam conditions. As briefly stated, two techniques were adopted: dynamic free vibrations monitoring and ultrasonic tests. The former test was carried out using 10 accelerometers located at relevant positions of the element, and an instrumented hammer as the impulsive force. The acquisition system is a NI PXI-1042Q, which allows to record the signal, that was further analyzed both in time and frequency domains through both Frequency Domain Decomposition (FDD) and Power Spectral Density (PSD) to derive the modal parameters necessary for the analysis. Ultrasonic tests were performed with successive tests located at nine different locations of the beam. Each test consists of a triplet of ultrasonic test, being one direct and two inclined, with the aim of covering the majority of the element surface. The signal acquisition was performed using PunditLink software.

Table 2. Load cycles for Beams 1, 2 and 3.

Cycle	Beam 1		Beam 2		Beam 3	
	kN	%	kN	%	kN	%
0	0	0	0	0	0	0
1	20	35.5	18.6	27.6	25.8	36.6
2	11.9	21.1	26.5	39.2	35.7	50.6
3	18.7	33.2	35.3	52.3	45.8	64.9
4	26.0	46.3	45.1	66.9	70.5	100.0
5	34.6	61.5	65.3	96.8	-	-
6	45.1	80.1	67.5	100.0	-	-
7	56.3	100.0	-	-	-	-

Table 3. Load cycles for (a) Beams 4, (b) 5 and (c) 6.

a)

Beam 4	Load		Prestressing	
	kN	%	kN	%
0	0	0	0	0
1	11	27.5	0	0
2	30	75	160	100
3	30	75	85	53,1
4	40	100	160	100
5	40	100	0	0

b)

Beam 5	Load		Prestressing	
	kN	%	kN	%
0	0	0	0	0
1	11	24.4	0	0
2	40	88.9	160	100
3	40	88.9	95	59.3
4	45	100	160	100
5	45	100	0	0

c)

Beam 6	Load		Prestressing	
	kN	%	kN	%
0	0	0	0	0
1	11	10.0	0	0
2	30	54.5	160	100
3	30	54.5	95	59.3
4	55	100	160	100
5	55	100	0	0

3 RESULTS

In the following figures the results are presented for dynamic and ultrasonic tests. In particular, fundamental frequencies and damping ratio were calculated from the recorded signals. In particular, the calculation of damping ratio was made directly on time histories, by interpolating the peaks of the free decay curve with a fitting algorithm and a model of pure viscous damping.

Results for Beams 1, 2 and 3 are summarized in Figure 4. As expected, a general decrease of fundamental frequencies and an increase in damping ratios with the increase of damage was detected. In percentage terms, the damping ratio is more sensible to prestressing force variation than the frequency, showing how the damping ratio represents a valid indicator of damage, as well as fundamental frequencies.

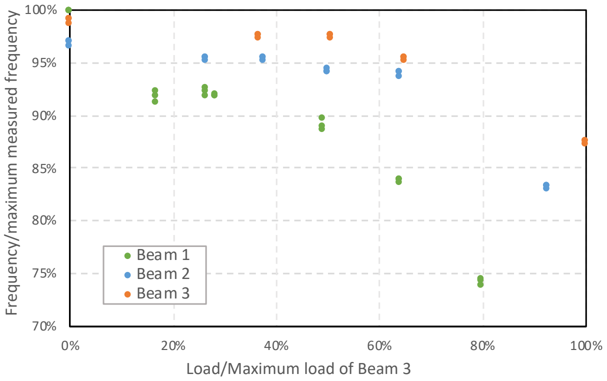

(a)

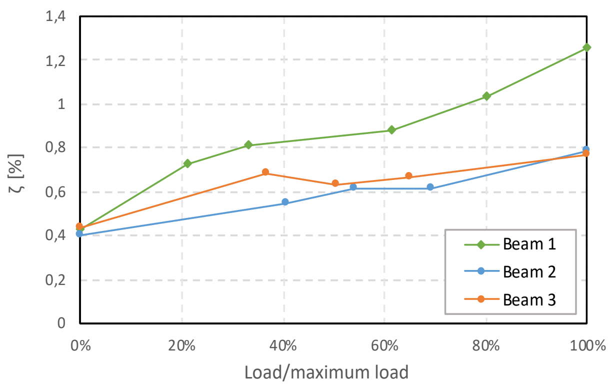

(b)

Figure 4. (a) Frequency variation – first mode; (b) damping variation

In Figure 5 the results of ultrasonic tests are shown in terms of map of velocity, obtained by an interpolation of crossed ultrasonic signal measured in a tomographic configuration. The picture shows an example of these maps for different damage levels, with a decrease of ultrasonic velocity with the increase of damage.

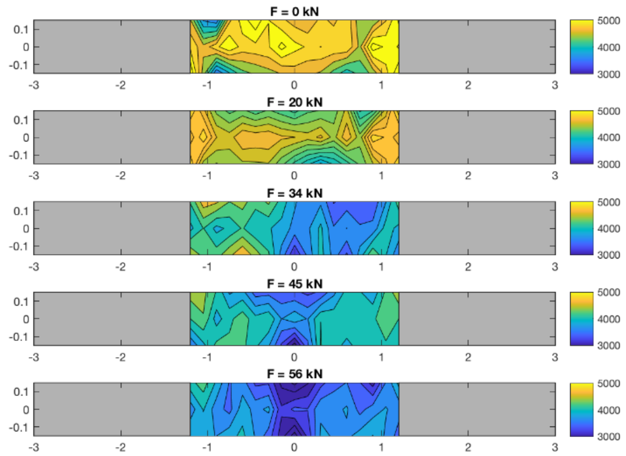

Figure 5. Beam 1: map of velocity for different damage states

4 RESULTS COMPARISON AND INTERPRETATION

The tests conducted on the beams with different amount of damage and different level of prestressing, showed how non-destructive parameters like fundamental frequencies, damping ratio and ultrasonic velocity are influenced by both of the above mentioned parameters. However, while the correlation between damage and fundamental frequency variation is widely recognized in literature, few models can be found that investigate the change in non-destructive parameters with the variation of prestressing force.

Starting from Eq.2, the theoretical fundamental frequencies of the six beams were calculated, and compared to the measured frequencies. It is worth to recall that the value of *EI* in Eq.2 was not assessed in terms of static parameters, but with the use of non-destructive data only; this approach gives the advantage of being exploitable for practical applications, where static parameters are usually unknown. For this reason, the authors made use of the estimation of ultrasonic velocity to calculate the dynamic Young Modulus, while the modulus of inertia was calculated by estimating the ratio L_{crack}/L, where L_{crack} is the length over which flexural cracking is expected to occur, and L is the overall length of the beam. Hence, this procedure does not involve the use of any experimental static measure.

In Figure 6, the comparison between experimental frequencies (in shades of blue) and theoretical frequencies (shades of red) are shown for Beams 1, 2 and 3. Darker lines represent higher level of damage.

Figure 7, 8 and 9 show the same comparison for Beam 4, 5 and 6, respectively. The use of post tensioned cables allowed to investigate a higher number of prestressing levels, varying the applied force to the cable through the hydraulic jack. For every beam, three levels of damage are studied: undamaged beam (blue line), cracked beam (orange line) and broken beam (grey line).

A good approximation of the model with experimental results was found, especially for post-tensioned beams. In particular, as seen from the pictures, the above-described procedure give a rough estimate of the trend of variation that was expected from experimental results, even if some difference is still evident for pre-tensioned beams.

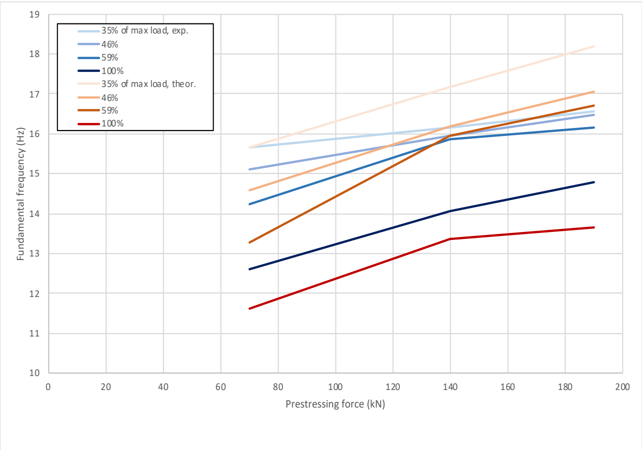

Figure 6. Variation of fundamental frequency with prestressing force for Beams 1, 2 and 3: comparison between experimental (shades of blue) and theoretical (shades of red) results.

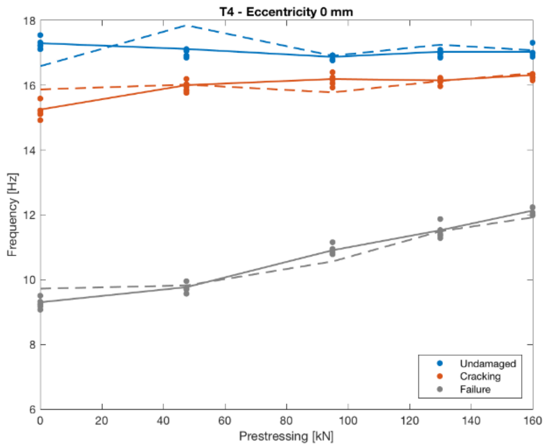

Figure 7. Variation of fundamental frequency with prestressing force: Beam 4.

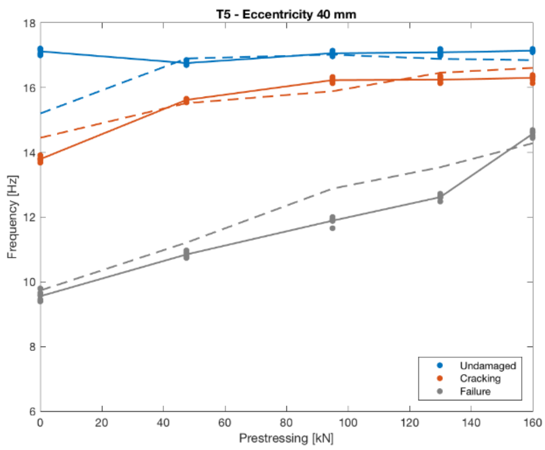

Figure 8. Variation of fundamental frequency with prestressing force: Beam 5.

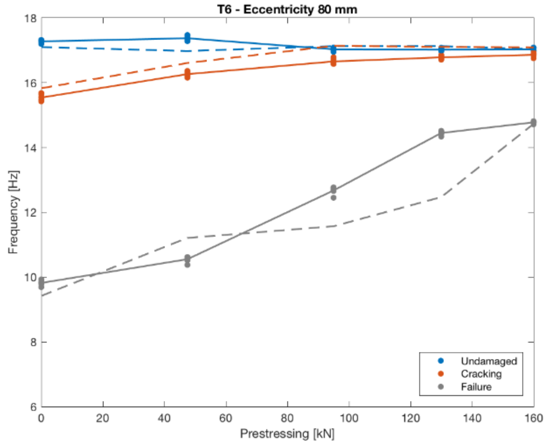

Figure 9. Variation of fundamental frequency with prestressing force: Beam 6.

5 CONCLUSIONS

In this paper the outcomes of an experimental campaign carried out on pretensioned and post-tensioned prestressed reinforced concrete (PC) beams are summarized, aimed at assessing the influence of varying prestress levels on both static and dynamic structural parameters.

Six PC beams, with different amount of prestressing force, were tested under bending tests, with increasing levels of applied load.

Non-destructive parameters, like fundamental frequencies, damping ratios and ultrasonic velocity were measured for every beam at different damage levels. Then, a procedure for the assessment of the theoretical fundamental frequencies of vibration was tested, that makes use of non-destructive parameters only to estimate the level of prestress in the beams. The procedure compared the fundamental frequencies experimentally measured with the theoretically estimated ones.

Results showed how the proposed procedure gives a rough estimation of the trend of the variability of fundamental frequencies both with increase of prestressing and with the evolution of damage, even with some difference with respect to the experimental results, mostly for pre-tensioned beams. Such discrepancy, however, should be better analyzed in further works. Indeed, it is believed that, with appropriate calibration, the method can be applied to a wide number of real structures, where the estimation of the residual amount of prestressing force can be a crucial parameter for the assessing of their health conditions.

REFERENCES

Cawley P. & Adams, R., 1979. The location of defects in structures from measurements of natural frequencies, *Journal Of Strain Analysis*, **14**(2), pp. 49-57.

Black P. and White P.G., 2009. Analysis at the Ultimate Limit State of a R/C Slab Supporting Desiccated-Sludge Silos, *European J. of Environmental and Civil Engineering*, **13**(6), 685-706.

Burka L.P., 1993. A hypertext history of multi-user dimensions. MUD history, *<http://www.ccs.neu.edu/home/1pb/mud-history.htm1>*

Fisher J.W. and Stroik J.H.A., 1974. Guide to design criteria for bolted and riveted joints, *Wiley*, New York.

International Conference of Building Officials – ICBO, 1997. *Uniform building code*, Whittier, California.

Kurtz M., 1991. Section 7: Transformation of space in computer graphics, *Handbook of applied mathematics for engineers and scientists*, McGraw-Hill, New York, 7.1-7.42.

Szilard R., 1974. Theory and Analysis of Plates: Classical and Numerical Methods. *Prentice Hall*, N.J.

Morazzini S., 2018. RC Slabs with Mixed Constraints: Ultimate Limit State and Fire (in Italian). MS Dissertation defended on July 25, 2018, at the Politecnico di Milano, 162 p.